Investigation on the physicochemical properties and antibacterial activity of pure and Zn doped CuO nanoparticles

L. Guru Prasad[a,*], T. Janeba[b], R. Ganapathi Raman[b]
[a]*Department of Science & Humanities, M. Kumarasamy College of Engineering, Karur, India*
[b]*Department of Physics, Noorul Islam University, Thuckalay -629175, India*

Pure and Zn doped CuO nanoparticles have been synthesized by co-precipitation method. Structural characterization reveals that the prepared materials are in monoclinic structure. Band gap value of the calculated from optical spectrum and it is observed band gap of the prepared materials gets decrease by increasing the concentration of dopant. It is evidently visible in SEM picture that the Zn doped CuO nanoparticles are nearly globular in form with identical size distribution. Antibacterial activity of the title materials have also been tested against *Acinetobacterbaumanni and Klebsiella pneumonia.*

(Received January 27, 2021, Accepted April 12, 2021)

Keywords: CuO, XRD, Morphology, Antibacterial activity

1. Introduction

Recently nanomaterials receive much attention among the researchers because of its potential applications in engineering and medicinal field. In the existing materials, transition metal oxide materials are much attracted because of its electrical properties. Properties of the metal oxide vary as their size changes and due to this large number of metal oxide nanoparticles have been synthesized and reported its semiconducting nature. In recent times, nanomaterials with biological applications are given much importance since it provides promising way to treat the human diseases [1]. Most of the nano materials' size matches with the size of the biological molecule hence it will be a good candidate to apply in the biological problems [2]. Simple copper oxide (CuO) has an unoccupied 3d-shell and it has enthralled uses when it is in nano size. Although the CuO have metallic nature in bulk form they act like semiconductor when the size becomes nano. As a result of its exceptional physical, chemical and biological properties, it is being used in many areas like in sensing devices, in antimicrobial activity and etc., [3]. With this knowledge, we tried to synthesis and to investigate the pure and Zn doped CuO nanoparticles for antibacterial activity applications.

2. Experiments

2.1. Materials and methods

2.1.1 Synthesis of pure CuO and Zn doped CuO

Synthesis of pure and Zn doped CuO nanoparticles have been carried out by co-precipitation method. About 39.93 g of copper acetate is taken in a conical flask and dissolved in the known quantity of deionized water. Parallelly, NaOH solution is prepared by using 8g of NaOH and which is added slowly in copper acetate solution. This mixture is stirred for 4 hr at constant temperature which yields CuO particles as precipitation.

To prepare Zn doped CuO, zinc acetate is added as 1, 2 and 3 mol% concentration in copper acetate solution and then it is added the solution of NaOH as mentioned above. The resultant precipitations are filtered out and washed in distilled water in to remove the non-reacted impurities. To remove the organic material, the precipitations are further purified by washing with

* Corresponding author: guruprasadl.snh@mkce.ac.in

methanol. Final products are kept in the oven for drying purpose at 150°C and the dried materials are calcinated at 400°C for 4 hrs in the closed atmosphere. Finally black powders are obtained with high purity [4-6]. The calcinated nanoparticles are used for further characterizations.

3. Characterization

Powder XRD pattern has been recorded for the prepared samples using XPERT-PRO X-ray diffractometer with CuK_α (λ = 1.54056 Å) radiation. The sample was examined over the range 10^o – 70^o at the rate of 1^o/min.. Vibrational spectrum has been documented using 8400S Shimadzu infrared spectrophotometer in the region 4000-400 cm^{-1}.

The UV–Vis spectrometer studies have been performed by Systronics, India. The particle size and surface morphology of the prepared nanoparticles particle were studied through Scanning Electron Microscope (SEM), and the images were recorded using Tescan vega3 sbu. The surface topography and near field optical imaging of the samples was determined by Atomic Force Microscopy (AFM) using XE70, Park Systems, Korea. Samples were also examined to antibacterial activity against two pathogenic bacteria Acinetobacterbaumanni and Klebsiella pneumonia.

3.1. Powder x-ray diffraction

The synthesized nanoparticles are confirmed by analyzing the Powder X-ray diffraction (PXRD) pattern. The PXRD patterns of pure CuO and with diverse concentrations of Zn doped (1, 2 and 3 mol %) nanoparticles are shown in Fig. 1.

Peaks were matched up with JCPDS card no. 89-5895 and indexed. No modification in the monoclinic structure of CuO is observed in the zinc doped samples. The average grain sizes of the synthesized samples are calculated by using Debye-Scherrer formula.

The grain size of the sample $D = \frac{0.9\lambda}{\beta cos\theta}$

where, D→Particle diameter

K→is a constant equal to 0.9
λ→wavelength of the X-ray source
β→ Full width half maximum (FWHM)
θ →half diffraction angle

The average grain size of the synthesized for pure, 1, 2 and 3 mol% Zn doped CuO nanoparticles found as 18.55 nm, 20 nm, 22 nm, and 20 nm respectively. XRD results it shows that below 20 nm smaller particles have high value of strain and greater the particles size have less value of strain. New peak with the (h k l) planes (1 1 2) and also existing peaks are narrowed in the angle of $42^\circ, 46^\circ, 68^\circ$ with (h k l) planes (2 0 0), (1 0 2), (1 2 2) confirms the presence of Zn in the doped CuO samples [7-10].

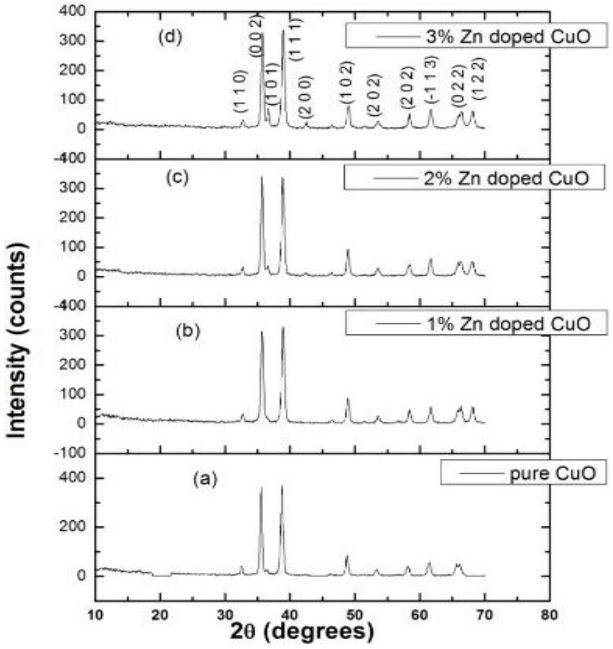

Fig. 1. XRD pattern of spectrum of Pure and Zn doped CuO nanoparticles

3.2. Fourier transform infrared spectroscopy (FTIR)

FTIR Spectrum is recorded in 8400S Shimadzu infrared spectrophotometer using KBr pellet technique in the frequency range 4000-400 cm^{-1} to recognize functional groups. Vibrational spectrum are presented in Fig. 2. Observed vibrational peaks are matched up to equivalent functional groups for the samples of pure CuO and various concentration (1, 2 and 3 mol%) Zinc doped CuO and given in Table 1.

Table 1. Observed vibrational wavenumber and their corresponding assignments.

Wavenumber (cm^{-1})				**Assignments**
Pure CuO	1 mol% Zn doped CuO	2 mol% Zn doped CuO	3 mol% Zn doped CuO	
2299.15	2299.15	2260.51	2268.29	Cu absorption band
-	-	1905.67	1905.67	ZnO Peak
1728.22	1735.93	1728.22	1728.22	O-H bending
1651.07	1643.35	1627.92	1627.92	O-H bending
1558.48	1558.48	1527.62	1527.62	CuO Peak
1458.18	1458.18	1458.18	1458.18	O-H bending
1373.32	1373.32	1373.32	1373.32	CuO Peak
1064.71	1064.71	1064.71	1064.71	Cu absorption band
-	-	995.27	995.27	Zinc oxide peak
586.36	586.36	578.64	578.64	Cu absorption band
	439.77	439.77	424.34	Zinc oxide band

Observed frequency and its corresponding assignments are tabulated in Table.4.5. Commonly metal oxide generally shows its absorption peak under 1000 cm^{-1} that taking place because of the inter-atomic vibration. In the current investigation this vibration is perceived at 995 cm^{-1}, 578 cm^{-1} and 424 cm^{-1}. The absorption peak at 2299 cm^{-1}, 1558 cm^{-1}, 1373 cm^{-1}, 1064 cm^{-1} and 586 cm^{-1} shows the presence of CuO, this supports the presence of monoclinic phase [11-15]. The absorbed band at 1458 cm^{-1}, 1728 cm^{-1}, 1651 cm^{-1} represents to O-H bending vibration [16],

the band at 1905 cm^{-1}, 995 cm^{-1} and 439 cm^{-1} indicates ZnO peak, this authenticate the existence of Zinc in the doped samples. Therefore it was assumed that the formation of plane take place depends on the synthetic methodology. It can be supported by XRD.

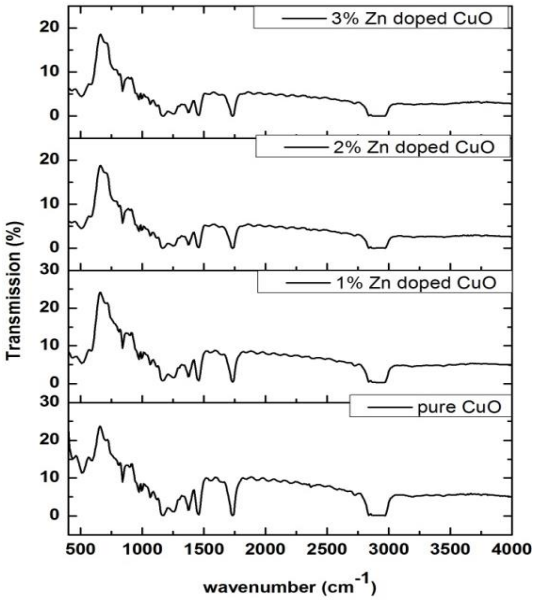

Fig. 2. FTIR spectrum of Pure and Zn doped CuO nanoparticles.

3.3 UV–Visible characterisation

UV–Vis absorption spectrum was recorded using Systronics, India in the wavelength range of 200 to 1100 nm. UV–Vis absorption spectrum for both pure and Zn (1, 2 and 3 mol %) doped CuO samples are presented in Fig. 3a. The absorption peak of pure CuO and Zn doped (1, 2 and 3 mol%) are 320 nm, 357 nm, 360 nm and 365 nm respectively. The direct band gap of the sample is calculated by plotting the graph between photon energy versus $(\alpha h\nu)^2$ and it is shown in Fig. 3b, the band gap energy values are found to be 3.6 eV and 3.3 eV for pure CuO and Zn doped with different concentration (1,2 & 3 mol%) in CuO. The band gap energy values are decreases while increasing doping concentrations. By reason of Burstein-Moss effect, there is an increase in electron concentration (due to Zinc doping) which leads a minute shift in the band gap [17-19].

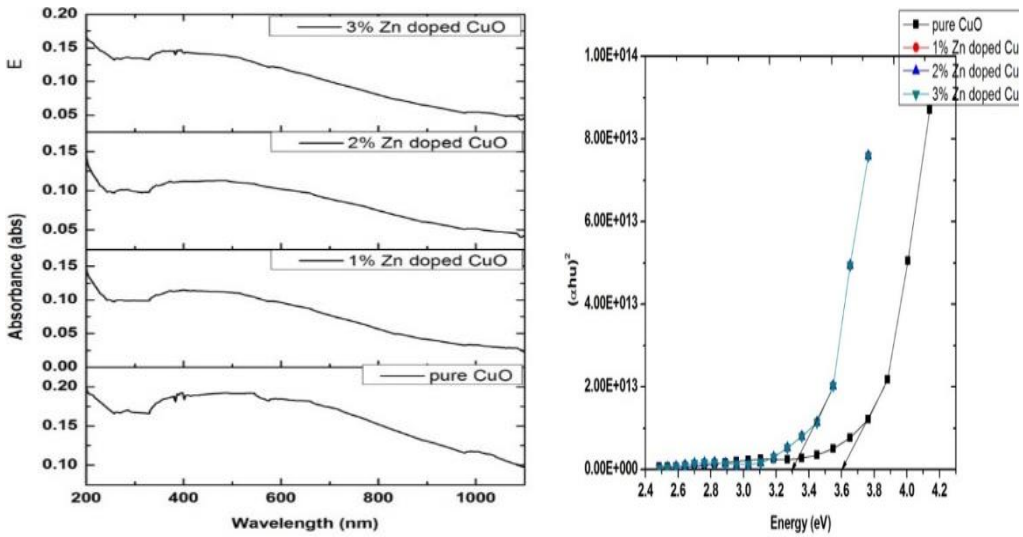

Fig. 3. (a) UV-VIS spectrum of pure and Zn doped CuO nanoparticles (b) $(\alpha h\nu)^2$ Vs Energy.

3.4. Scanning electron microscopy (SEM)

Samples are analyzed through Tescan vega3 SBU Scanning electron microscope, it is employed to analyze the surface morphology and the growth features of the aggregates of the prepared nanoparticles. Scanning electron micrograph of synthesized CuO nanoparticles and Zn doped CuO nanoparticles are shown in Fig. (4a-4d). Larger percentage of agglomerations is noticed in the SEM image of the pure sample. It is also noticed that the doped are nearly sphere-shaped with harmonized size distribution. Presence of dopant Zn does not alter the morphology of CuO and it is observed from SEM images that sample addition of a certain amount of dopant zinc to the pure CuO led to the formation of spongy and fragile Zn-CuO material containing voids and pores. This could be recognized to during the liberation of huge quantity of gases in the combustion process. The pores/voids between the grains also decrease with Zn concentration. The observable fact of "nuclear-aggregation" is caused by the swift development of crystal nucleus [20-21]. The rate of occurrence this aggregation is a key component that manages the morphology and structure of the materials [22].

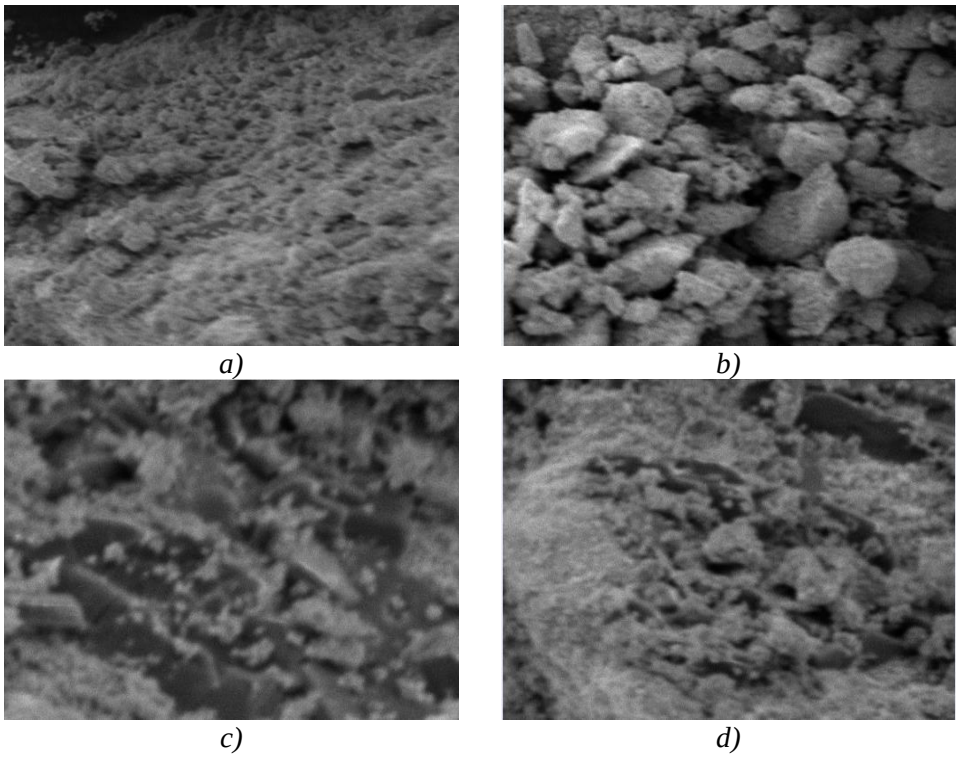

Fig. 4. SEM image of CuO nanoparticles
a) pure CuO, b) Zn (1 mol%) doped CuO, c) Zn (2 mol%) doped CuO, d) Zn (3 mol%) doped CuO

3.5. Atomic Force Microscopy (AFM)

The surface topography and near field optical imaging of the samples was recorded by Atomic Force Microscopy (XE70, Park Systems) Korea**.** Fig. 5a shows the AFM image of pure CuO. Fig. 5b is the histogram of pure CuO it clearly shows that the prepared particle high uniformity of the particles. The AFM image of Zn doped CuO is shown in Fig. 5c, while adding the dopant zinc caused the increasing of the size of the grains. It also revealed that it consists of clusters of round-shaped grains; this is due to the presence of Zinc. The mobility and the migration also increase by adding the dopant zinc resulting in the large grains. We can see the slight variation in the Zinc doped CuO Histogram and it is shown in Fig. 5d. This is due to the defect caused by adding Zn concentration.

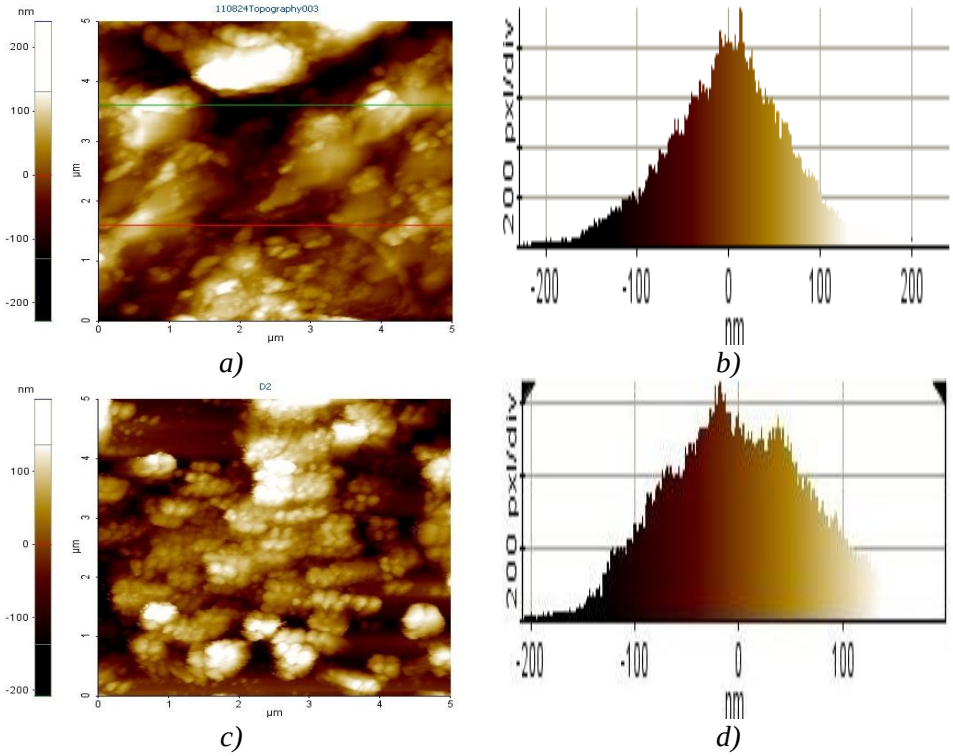

Fig. 5. a) AFM image of Pure CuO.
b) Histogram of Pure CuO.
c) AFM image of Zn doped CuO.
d) Histogram of Zn doped CuO.

3.6. Antibacterial activity

Pure CuO and Zn doped (1, 2 and 3 mol%) CuO nanoparticles were undergone to antibacterial activity for two pathogenic bacteria namely *Acinetobacterbaumanni* and *Klebsiella pneumonia*. Fig. 6a and 6b shows the antibacterial image of pure CuO and Zn doped CuO. Table 4.9 Antibacterial of pure CuO and Zn doped (1, 2 and 3 mol%) CuO. In order to test the antimicrobial activity against pathogenic organisms, well diffusion test was perfomed on nutrient agar and Czapek-Doxagar plates. Nutrient Agar Medium (NAM) was set up with pH 6.8-7.0 and transferred in the sterile petriplates. This was solidified with the bacterial suspension. Over this surface, 50 µl of prepared nanoparticles solution were poured and the inhibition zones were noticed, after the incubation period of 3 to 5 days. Results of the antimicrobial test performed for Pure CuO and Zn doped (1, 2 and 3 mol%) CuO nanoparticles in the way mentioned above and the result are tabulated in the Table. 2. From the Table. 2, it is recognized that both the pure and doped sample have better activity against the pathogens [23]. Hence Zn-doped CuO nanoparticles can be used in pharmaceuticals to prepare alternate anti-drug against pneumonia.

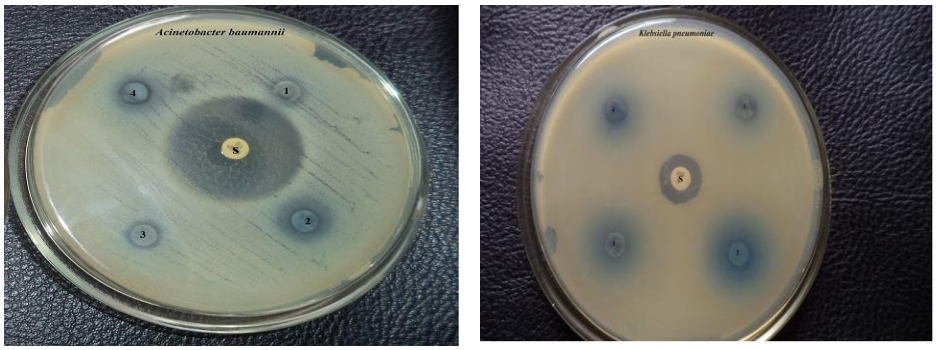

a) *b)*

Fig. 6. A) Antibacterial of pure CuO and Zn doped (1, 2 and 3 mol%) CuO.
b) Antibacterial of pure CuO and Zn doped (1, 2 and 3 mol%) CuO.

Table 2. Antibacterial of pure CuO and Zn doped (1, 2 and 3 mol%) CuO.

S.No	Type of nanoparticles	Diameter of Inhibition Zone	
		Acinetobacterbaumanni (Std.A 36)	Klebsiella pneumonia (Std.A 16)
1	CuO	13	14
2	1 mol% Zn doped CuO	_	11
3	2 mol% Zn doped CuO	10	10
4	3 mol% Zn doped CuO	_	10

4. Conclusions

Using co-perception method the pure and Zn doped CuO nanoparticles have been synthesized and the prepared materials were confirmed by the analyzing the XRD spectrum. There is minute band gap value shifts are noticed in the doped samples. Prepared materials are almost spherical in shape and due to increase in electron concentration agglomeration are noticed in the doped samples. Antibatcterial activity of both the samples was tested against Acinetobacterbaumanni and Klebsiella pneumonia and confirms both the samples are doing well against the pathogens.

References

[1] Wanisa Abdussalm-Mohammed, Advanced Journal of Chemistry Section A: theoretical, Engineering and Applied Chemistry **3**, 192 (2020).
[2] D. Manyasree, Kiran May Peddi, R. Ravikumar, International Journal of Applied Pharmaceutics **9**, 71 (2017).
[3] V. Bhuvaneswari, D. Vaidehi, S. Logpriya, Microbiol. Curr. Res. **2**, 9 (2018).
[4] K. Z. Nia, M. Montazer, Physicochemical and Engineering Aspects **439**, 167 (2013).
[5] M. M. Rahman, S. Bahadar Khan, A. M. Asiri, H. M. Marwani, A. H. Qusti, Composites Part B: Engineering **54**, 215 (2013).
[6] K. Mageshwari, R. Sathyamoorthy, Journal of Material Science and Technology **29**, 909 (2013).

[7] Q. Hao, H. Maa, Z. Jua, G. Li, X. Li, L. Xua, Y. Qiana, Electrochimica Acta. **56**, 9027 (2011).
[8] C. C. Vidyasagar, Y. Arthoba Naik, T.G. Venkatesh, R. Vishwanatha, Journal of Powder Technology **214**, 317 (2011).
[9] F. Bayansal, S. Kahraman, G. C. Ankaya, H. A. C. Etinkara, Journal of Alloys and Compounds **509,** 2094 (2011).
[10] F. Bakhtiari, E. Darezereshki, Mater. Lett. **65**, 171 (2011).
[11] D. W. Zhang, C. Chen, J. Zhang, F. Ren, Journal of Material Science **43**, 1492 (2008).
[12] X. C. Zheng, S. P. Wang, S. R. Wang, S. M. Zhang, W. P. Huang, S. H. Wu, Materials Science and Engineering **25**, 516 (2005).
[13] A. Viano, S. R. Mishra, R. Lloyd, J. Losby, T. Gheyi, Journal of Non-Crystalline Solids **325**, 16 (2003).
[14] S. Ohyama, H. Kishida, Applied Catalysis A: General **184**, 239 (1999).
[15] M. Guedes, J. M. F. Ferreira, A. C. J. Ferro, Colloid Interface Science **330**, 119 (2009).
[16] D. Fernandes, R. Silva, A. Winkler Hechenleitner, E. Radovanovic, M. Custydio Melo, E. Pineda, Mater. Chem. Phys. **115**, 110 (2009).
[17] J. I. Pankove, Optical Properties in Semiconductor, Prentice Hall, Englewood Cliffs, NJ, 1971.
[18] H. Wei, M. Li, Z. Ye, Z. Yang, Y. Zhang, Mater. Lett. **65**, 427 (2011).
[19] R. Pino, Y. Ko, P. S. Dutta, Burstein, Journal of Applied Physics **96**, 5349 (2004).
[20] Siquingaowa, Zhaorigetu, H. Yao, Garidi, Frontiers of Chemistry in China **3**, 277 (2006).
[21] F. Zhang, J. Yang, International Journal of Chemical Kinetics **1**, 18 (2009).
[22] Z. C. Michael Hu, T. Michael Harris, H. Charles Byers, Journal of Colloid and Interface Science **198**, 87 (1998).
[23] M. Suleiman, M. Mousa, A. Hussein, B. Hammouti, Taibi B. Hadda, I. Warad, Journal of Materials and Environmental Science **4**, 792 (2013).